Biocalcification of Sand through Ureolysis

Chiung-Wen Chou[1]; Eric A. Seagren, A.M.ASCE[2]; Ahmet H. Aydilek, M.ASCE[3]; and Michael Lai[4]

Abstract: Biological processes may provide great and previously unexplored opportunities for cost-effective, in situ improvement of the engineering properties of soil. A laboratory study was conducted to evaluate the changes in geomechanical properties of sand attributable to the formation of calcium precipitates induced through ureolysis catalyzed by *Sporosarcina pasteurii* (*S. pasteurii*). Specifically, direct shear and California Bearing Ratio (CBR) tests were conducted on sand specimens subjected to treatment by growing, resting, and dead *S. pasteurii* cells in completely stirred tank reactors and completely mixed biofilm reactors, respectively. Scanning electron microscopy analyses were also conducted to evaluate microbially induced precipitation. The results of the study show that the bacterial cells effectively improved the geomechanical properties of the sand. Growing cells improved the sand properties owing to microbially induced precipitation and related pore volume changes, whereas dead and resting cells generally caused smaller increases in friction angle and bearing strength. Analysis of the sand from CBR specimens treated with growing cells demonstrated that the microbial and chemical processes both contributed to the clogging of the porous medium. **DOI: 10.1061/(ASCE)GT.1943-5606.0000532.** © *2011 American Society of Civil Engineers.*

CE Database subject headings: Soil properties; Bacteria; Calcium carbonate; Soil strength; Sand (soil type).

Author keywords: Soil properties; Bacteria; Calcium carbonate; Strength.

Introduction

Microbial activities are ubiquitous in surface and subsurface soils and have a tremendous effect on the composition, properties, and geomechanical behavior of earth materials [National Research Council (NRC) 2006]. Examples of biomediated processes that have been investigated for their influences on geomechanical properties include mineral precipitation, biofilm formation, use of biopolymers, mineral transformation, and biogenic gas production (Seagren and Aydilek 2009). For example, natural cementation of geological formations through mineral precipitation occurs constantly over time owing to physiochemical and microbiological reactions. These microbially mediated reactions result in relatively insoluble compounds that can contribute to soil cementation. One of these natural processes is microbially induced calcium carbonate ($CaCO_3$) precipitation.

Microbially induced $CaCO_3$ precipitation, or biocalcification, is a ubiquitous process and plays an important cementation role in natural systems including soils, sediments, and minerals (Buczynski and Chafetz 1991; Monger et al. 1991; Defarge et al. 1996). As reviewed by Seagren and Aydilek (2009), examples of heterotrophic processes (i.e., processes in which microbial cells obtain their carbon from organic compounds) associated with biocalcification include biotransformation of organic nitrogen compounds, e.g., urea hydrolysis (Gollapudi et al. 1995; Stocks-Fischer et al. 1999; Urzi et al. 1999; Fujita et al. 2000; Ramachandran et al. 2001; Ross et al. 2001; Bang et al. 2001; DeJong et al. 2006; Whiffin et al. 2007), and oxidation of organic compounds under denitrifying (Abdelouas et al. 1998; Karatas et al. 2008), sulfate-reducing (Abd-El-Malek and Rizk 1963; Van Lith et al. 2003; Aloisi et al. 2006), and methanogenic (Rittmann et al. 2003; VanGulck et al. 2003) conditions. In addition, chemosynthetic and photosynthetic autotrophs (i.e., organisms that use CO_2 as their carbon source) can induce the precipitation of carbonates when they remove CO_2 from bicarbonate-containing solutions in the presence of an adequate supply of Ca^{2+} or other appropriate cations (Ehrlich 2002), such as during hydrogenotrophic methanogenesis (i.e., formation of methane and conversion of hydrogen to other compounds) (Castanier et al. 1999), autotrophic denitrification (Lee and Rittmann 2003), and photosynthesis in the open, aerobic environment (Thompson and Ferris 1990).

Among the different mechanisms of biocalcification, urea hydrolysis (or ureolysis), as shown in Eq. (1), was the focus of the work reported in this paper:

$$\begin{aligned} &NH_2CONH_2 + 3H_2O \xrightarrow{\text{Urease}} 2NH_4^+ + CO_2 + 2OH^- HCO_3^- \\ &+ OH^- \leftrightarrow H_2O + CO_3^{2-} \cdot CO_3^{2-} + H_2O \leftrightarrow 2OH + CO_2 \end{aligned} \quad (1)$$

The release of NH_4^+ and CO_2 results in an increase in pH and alkalinity, thereby creating an environment in which at least some of the CO_2 produced will be transformed into carbonate. Thus, in unbuffered environments containing adequate amounts of Ca^{2+} and other cations, $CaCO_3$ precipitation can result if the solubility product, K_{sp}, is exceeded (Sawyer et al. 2003):

$$\begin{aligned} &CaCO_3(s) \leftrightarrow Ca^{2+} + CO_3^{2-} \\ &K_{sp} = [Ca^{2+}][CO_3^{2-}] = 5 \times 10^{-9}\ \text{mole}^2/\text{L}^2 \quad \text{at } 25°\text{C} \end{aligned} \quad (2)$$

Biocalcification likely occurs through a combination of homogeneous and heterogeneous nucleation (Mitchell and Ferris 2006).

[1]Graduate Research Assistant, Dept. of Civil and Environmental Engineering, Univ. of Maryland, 1163 Glenn Martin Hall, College Park, MD 20742.

[2]Associate Professor, Dept. of Civil and Environmental Engineering, Michigan Technological Univ., 1400 Townsend Dr., Houghton, MI 49931.

[3]Associate Professor, Dept. of Civil and Environmental Engineering, Univ. of Maryland, 1163 Glenn Martin Hall, College Park, MD 20742 (corresponding author). E-mail: aydilek@umd.edu

[4]Graduate Research Assistant, Fischell Dept. of Bioengineering, 2334 Jeong H. Kim Engineering Building, Univ. of Maryland, College Park, MD 20742.

Note. This manuscript was submitted on July 10, 2009; approved on March 10, 2011; published online on March 12, 2011. Discussion period open until May 1, 2012; separate discussions must be submitted for individual papers. This paper is part of the ***Journal of Geotechnical and Geoenvironmental Engineering***, Vol. 137, No. 12, December 1, 2011. ©ASCE, ISSN 1090-0241/2011/12-1179–1189/$25.00.

Homogeneous carbonate nucleation results when the heterotrophic and autotrophic metabolic processes discussed previously cause changes that lead to oversaturation in the bulk solution chemistry and in microenvironments surrounding cells, thereby catalyzing precipitation (Schultze-Lam et al. 1996). Heterogeneous nucleation occurs when bacterial cells (living or dead) function as nucleation sites (Schultze-Lam et al. 1996), through the binding of cations to the wall (Greenfield 1963; Stocks-Fischer et al. 1999; Van Lith et al. 2003; Aloisi et al. 2006) and extracellular polymeric substances (EPS) (Braissant et al. 2007; Ercole et al. 2007), both of which carry a net negative electric charge. For example, if free Ca^{2+} is available, the conditions are favorable for it to attach to cells because of the attractive force between the cations and the negatively charged cells (Stocks-Fischer et al. 1999):

$$Ca^{2+} + \text{Cell} \rightarrow \text{Cell} - Ca^{2+} \tag{3}$$

In the presence of carbonate, $CaCO_3$ precipitates form on the cells according to

$$\text{Cell-}Ca^{2+} + CO_3^{2-} \rightarrow \text{Cell} - CaCO_3\downarrow \tag{4}$$

Under in situ soil and aquifer conditions, the porous medium provides additional sites for nucleation on the matrix mineral surfaces (Ferris et al. 2004).

The biocalcification process, especially with use of urea as a microbial substrate, has been successfully implemented in the laboratory for improvement of sands and plugging of fractured rocks (Gollapudi et al. 1995; Urzi et al. 1999; Ramachandran et al. 2001; Ross et al. 2001; Bang et al. 2001; Day et al. 2003; DeJong et al. 2010). Nevertheless, the relationship between ureolysis and soil geomechanical properties is still not well understood in terms of the conditions necessary to stimulate these natural processes in situ, and the magnitude of the effects on soil properties. Therefore, this study investigated biocalcification in sand through ureolysis under biotic (with growing cells or resting cells, i.e., living cells in the absence of growth substrates) and abiotic (with dead cells or no cells) conditions. The effects of cell numbers and soil compaction on microbial cementation and the geomechanical properties of the sand, including improvements in soil strength and changes in hydraulic conductivity, were also examined. A key aspect of this study was the development of unique, dual-purpose experimental equipment that could serve as a bioreactor and be used directly in the testing equipment for determining the geomechanical properties of the specimen.

Materials and Methods

Sand

Unground silica sand (99.7% quartz) (U.S. Silica Company, West Virginia) was used in the experiments. The sand was uniformly graded (coefficient of uniformity, $C_u = 1.1$), had a median particle size (D_{50}) of 0.46 mm, and included no fines. It was classified as poorly graded sand on the basis of the Unified Soil Classification System. Microscopic analysis indicated that the sand was subangular in shape (Krumbein 1941). The specific gravity and pH of the sand were 2.65 and 6.5, respectively. The maximum and minimum void ratios determined per ASTM D4254 and D4253 were 0.93 and 0.68, respectively. Before use, the sand was sequentially washed with an acidic solution (0.25 N HCl) followed by a basic solution (0.25 N NaOH), each for 12 h with periodic stirring. Subsequently, the sand was rinsed with deionized water until a pH 7 was reached, and it was then autoclaved.

Microorganism

The bacterium used in this study was *Sporosarcina pasteurii* (*S. pasteurii*) [American Type Culture Collection (ATCC) 11859]. *S. pasteurii* 11859 was maintained on *Bacillus pasteurii* urease (BPU) medium (Bang et al. 2001) streak plates and refrigerated at 4°C. The culture was transferred monthly to fresh plates. To prepare the live cell inocula for the geomechanical tests with growing or resting cells, as described subsequently, a colony of *S. pasteurii* 11859 was aseptically transferred to 5 mL of autoclaved Tris-YE medium (Stocks-Fischer et al. 1999). The culture was incubated overnight at 30°C with shaking, and the cells were harvested during the late exponential phase as determined through absorbance ($\lambda = 600$ nm) in a spectrophotometer (Spectronic 21, Bausch & Lomb). This initial culture was then transferred aseptically to 1 L of Tris-YE medium, and the process was repeated. Next, the cells were harvested by centrifugation at 4,500 rpm for 10 min, after which the cell pellets were washed twice in 0.13 M Tris-HCl buffer (pH = 9). After washing, the cells were resuspended in the buffer to create a sufficient volume of cell suspension for the experimental systems described subsequently, at the desired concentrations of 10^3 and 10^7 colony-forming units (cfu)/mL on the basis of a correlation curve between absorbance at 600 nm and cell number. Alternatively, for the preparation of dead cells, a 1 L cell solution containing 10^8 cfu/mL was autoclaved for 30 min per day on three consecutive days. Then, this autoclaved cell suspension was diluted into the required volume of buffer at the desired cell concentrations.

Specimen Preparation

Model porous medium specimens were prepared using two experimental systems designed to promote uniform calcium carbonate formation within the pore spaces and allow key geotechnical properties (e.g., shear strength and bearing capacity) to be evaluated. Specifically, direct shear and California Bearing Ratio (CBR) tests were conducted on specimens prepared in completely stirred tank reactors (CSTRs) and hydraulically completely mixed biofilm reactors (CMBRs), respectively. In both reactor systems, the experimental conditions tested included (1) various cell types (i.e., growing, resting, and dead cell treatments); (2) different bacterial concentrations (i.e., 10^3 and 10^7 cfu/mL); and (3) two levels of compaction, i.e., loose- or dense-sand compaction at relative densities of 35% ($\gamma_d = 14.1$ kN/m^3) or 85% ($\gamma_d = 15.2$ kN/m^3), respectively.

CSTR System and Direct Shear Tests

The CSTR was created from a 6-L plastic tub covered with aluminum foil with silicone tubing for the influent and effluent lines, two peristaltic pumps to control the flow rates, a magnetic stir bar/mixer to provide mixing, and an air diffuser connected with filtered house air for aeration [Fig. 1(a)]. All components of the CSTR were sterilized by placement in a 0.1% HNO_3 acid bath for 24 h and rinsed with deionized water, followed by autoclaving.

To avoid possible reactions (e.g., corrosion) between conventional metal shear boxes and the aqueous media, shear boxes (100 × 100 mm) were constructed from polyurethane. These were sterilized before use by following the procedure described previously for the CSTR and were subsequently filled with sterilized sand. For the loose density, a funnel was used to aseptically pluviate the sand from 2 mm above the surface. Dense compaction was obtained by pluviating the sand from 0.3 m above the surface in four layers, with tamping after the introduction of each layer, following the procedures outlined in Abdulla (1995).

J. Geotech. Geoenviron. Eng., 2011, 137(12): 1179-1189

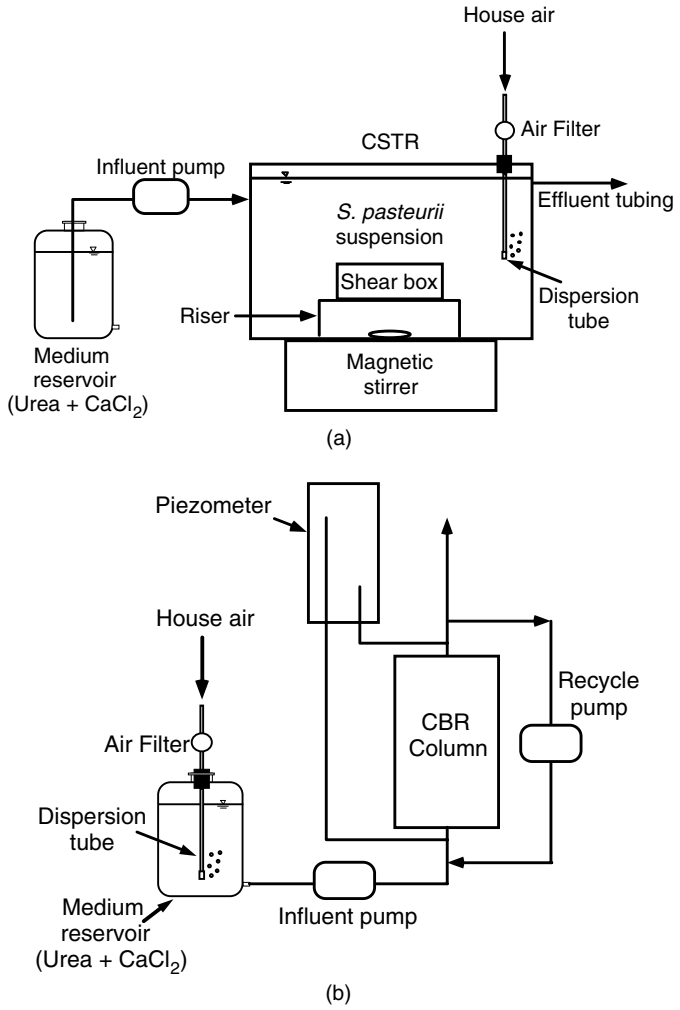

Fig. 1. Schematic drawings of: (a) CSTR/direct (i.e., lowercase) shear boxes system; (b) CMBR/CBR system

For each growing-cell experiment, triplicate shear boxes with loose or dense compaction were aseptically placed in the CSTR along with 6 L of live cell suspension (10^3 or 10^7 cfu/mL) [see Fig. 1(a)]. To ensure the shear boxes were inoculated, 3 L of the inoculum was poured equally through the boxes, which were then left undisturbed for 24 h to allow bacteria to attach to the sand particles. Subsequently, an aseptically prepared urea-$CaCl_2$ growth medium (nutrient broth 3 g, urea 20 g, NH_4Cl 10 g, $NaHCO_3$ 2.12 g, and $CaCl_2$ 2.8 g per liter of solution; final pH = 8.0) (Stocks-Fischer et al. 1999) was fed at flow rates of 9.5 or 8.3 mL/min for the specimens with loosely or densely compacted sand, respectively, corresponding to hydraulic retention times (HRTs) of 10.5 and 12 h. Conservative (bromide) tracer studies confirmed that complete mixing of the aqueous phase was achieved under these conditions (Chou 2008). Flow was continued until the monitored parameters (pH, urea, calcium, and cell number) approached a steady state. During this time, the direct shear specimens were in contact with the urea-$CaCl_2$ medium, but the medium was not forced to flow directly through the boxes. For the resting and dead cell treatments, the direct shear specimens with loose or dense compaction were placed in 6 L of the live or dead cell suspension (10^3 or 10^7 cfu/mL), respectively, for 24 h with complete mixing, but without addition of the urea-$CaCl_2$ medium.

After preparation in the CSTR, the shear strength of the specimens was determined using a direct shear apparatus. Multiple single-point direct shear tests [ASTM D3080 (ASTM 2005)] were conducted under normal stresses ranging from 11 to 40 kPa, and the specimens were kept saturated during the tests. Low normal stresses were applied to simulate conditions in contaminated material capping and unpaved road applications (e.g., biocalcification for dust control). A shear rate of 1%/min was utilized, and residual shear strength was measured when the shear box reached its displacement limit of 15 mm.

CMBR System and CBR Tests

The CMBR system included a PVC column (152 mm long, 152 mm in diameter), with top and bottom plates made of polyurethane board [see Fig. 1(b)]. All experimental conditions used in the CSTR system were also adopted for the CMBRs. To simulate loose compaction, the sterilized columns were prepared by aseptically pouring the sand from a funnel at a height of 2 mm above the surface. Dense compaction was achieved by pluviating the sterilized sand from 0.45 m above the sand surface in four layers, with tamping after introduction of each layer until the target dry density was achieved. Head loss across the column was measured by using a piezometer constructed from 305-mm-long glass tubing, attached to the system, and placed on a board adjacent to the column. The head loss across the column and flow rate were used with Darcy's law to determine the hydraulic conductivity. All components of the CMBR system were sterilized by autoclaving before use.

For each experiment with growing cells, the specimen with the selected density was saturated with 0.13 M Tris-HCl buffer at a flow rate of 1.5 mL/min for 24 h, after which the column was inoculated by pumping in 2 L of a suspension containing 10^7 cfu/mL live cells. The column then sat stagnant for 12 h to allow organisms to attach to the sand. Subsequently, the urea-$CaCl_2$ medium, which was aerated with filtered house air, was fed into the column. A peristaltic pump controlled the influent rate, Q, at 1.5–0.1 mL/min to provide an HRT of 12 and 10.5 h for the dense- and loose-compaction conditions, respectively. Another peristaltic pump was used to recycle the column effluent back to the influent at a recycle flow, Q_R, of 20 mL/min, giving a Q_R/Q ratio of 13. According to nonreactive tracer (bromide) studies, this resulted in approximately hydraulically completely mixed conditions in the columns (Chou 2008). Key parameters (urea, ammonium, calcium, pH, flow rate, dissolved oxygen, and cell number) were monitored until flow could no longer be generated through the column by the peristaltic pump. Preparation of the specimens with resting and dead cells followed the same procedure as preparation of the specimens with growing cells; however, live and dead cell inoculum concentrations of 10^3 and 10^7 cfu/mL, respectively, were used, and no substrate was supplied to prevent cell washout and growth of the resting cells.

Immediately after preparation, the CBR column was drained for a few minutes and the CBR tests were carried out at a 1.27 mm/min strain rate by using the Geotest Instrument S5840 Multi-Loader loading frame. Applied stress was 12 kPa to simulate low stresses in typical capping and unpaved road applications. All CBR tests were conducted by following the methods outlined in AASHTO T-193 and ASTM D1883.

Volatile and Mineral Film Analysis

Following the approach of Rowe et al. (2002), the material accumulated on the surface of the porous media in the CMBR was conceptualized as composed of a volatile biofilm containing active and inactive biomass and an inorganic solid film consisting of precipitated material. The biofilm thickness and density were estimated by

J. Geotech. Geoenviron. Eng., 2011, 137(12): 1179-1189

following the procedures described in Seagren et al. (2002). First, two samples of the sand, one from the top of the column and the other from the bottom, were aseptically removed from the CMBR with dense sand (inoculated with growing cells at 10^7 cells/mL) after deformation in the CBR measurement. The samples were stored in sterilized jars at 4°C until analyzed. The mass of water contained in the biofilm, W (M), was quantified by determining the mass loss attributable to drying (105°C) of the subsamples. Then the biofilm thickness, $L_{f,a}$ (L), was estimated by using the following equation:

$$L_{f,a} = \frac{W}{\rho n A(0.99)} \tag{5}$$

where ρ = water density at 20°C ($\mathrm{M\,L^{-3}}$); n = number of dry sand particles in the subsample; A = surface area of a sand particle ($\mathrm{L^2}$); and 0.99 = assumed fraction of the biofilm mass that is water. In this work, n was estimated by dividing the dry weight of the sand in the subsample by the mass per sand particle, which was estimated by multiplying the specific gravity of the sand by the volume of a sand particle, assuming that the particle is a sphere with the median diameter of a sand particle ($D_{50} = 0.46$ mm). Similarly, the surface area, A, was also calculated by assuming a spherical sand particle with a diameter equal to D_{50} and applying a correction factor of 1.3 for angularity per Russell and Taylor (1937) (i.e., the particles were subangular in shape).

The volatile solids (VS) weight, B (M), of the subsamples was used to estimate the biomass weight and was determined by measuring the mass loss of the dried subsamples attributable to ignition (550°C). Biofilm density, $X_{f,a}$ ($M_x\mathrm{L^{-3}}$), was then estimated according to the following equation:

$$X_{f,a} = \frac{B}{nAL_f} \tag{6}$$

Similarly, the thickness of the inorganic solid film, $L_{f,i}$ (L), was estimated by using the following equation adapted from Rowe et al. (2002):

$$L_{f,i} = \frac{B_{\mathrm{CaCO_3}}}{nAX_{f,i}} \tag{7}$$

where $B_{\mathrm{CaCO_3}}$ (M) = precipitated mass of Ca on the sand particles (reported as $\mathrm{CaCO_3}$) measured in the subsamples, and $X_{f,i}$ = inorganic solid film density ($M\mathrm{L^{-3}}$), which was assumed to be that of calcite = 2.71 $\mathrm{g/cm^3}$ (Roberts et al. 1990).

Scanning Electron Microscopy and Energy Dispersive X-ray Spectroscopy

Scanning electron microscopy (SEM) was used to examine the formation of microbially induced precipitation and biofilms on the surface of the sand matrix. Untreated sand and specimens preserved after treatment in the CMBR were first oven-dried at 40°C for three days. Subsequently, some specimens went through a pretreatment procedure, followed by mounting and coating, whereas other specimens were directly mounted and coated for SEM analysis without pretreatment to avoid dissolution of the authigenic minerals (i.e., minerals formed in situ). The pretreatment, mounting, and coating procedures are described in Chou et al. (2008). Once the specimens were coated, they were ready for SEM and semiquantitative energy dispersive x-ray spectroscopy (EDS) analyses.

Analytical Methods

Bromide was measured by using a bromide combination electrode (Orion 94-35, Thermo Electron Corp.) and an ion meter (Orion Model 520A). Readings (mV) were converted to $\mathrm{Br^-}$ concentrations on the basis of standard curves produced using dilutions of a bromide standard solution (1 ppm to 1,000 ppm).

The colorimetric method of Jung et al. (1975) was used to determine the aqueous urea concentration. To perform the test, a 50-μL sample was added to a test tube containing 2.5 mL of *o*-phthalaldehyde reagent, followed by 2.5 mL of naphthylenediamine reagent. The mixture was vortex mixed and incubated at 37°C for 30 min for the color development. A blank was prepared by adding 2.5 mL of BRIJ 35 (Ricca Chemical), instead of 50 μL of sample, and used to zero the spectrophotometer. Additionally, a reagent blank was prepared by adding 50 μL of deionized water. The absorbance of each tube was then recorded by using the spectrophotometer at a wavelength of 505 nm. A calibration curve of urea concentration versus absorbance values, which were corrected by subtracting the absorbance of the reagent blank, was prepared following the same procedures.

Calcium concentrations in aqueous samples were measured by using the ethylenediaminetetraacetic acid (EDTA) titration method, implemented in Method 3500-Ca [American Public Health Association (APHA) 1995]. The mass of calcium precipitates accumulated on the sand was determined as follows. First, subsamples of the porous media samples taken from the CMBR for determination of the biofilm thickness and density (see previous description) were dried at 105°C for 24 h, cooled, and weighed to get the mass of dry sand. The dry samples were rinsed with an acid solution of 0.1 N $\mathrm{H_2SO_4}$ to allow the precipitates to dissolve into the liquid phase. The sample plus solution was mixed by hand for 10 min and filtered through 0.45-μm filter paper, after which the calcium content was determined by using the EDTA titration method. This value was assumed to represent the content of calcium associated with the porous media and was converted to the equivalent mass as $\mathrm{CaCO_3}$ to give $B_{\mathrm{CaCO_3}}$.

Cell enumeration (cfu/mL) was performed by serial dilution in a 0.85% NaCl solution and spread plating on agar plates prepared using the urea-$\mathrm{CaCl_2}$ growth media. The number of cfu on the agar plates was counted after two days of incubation at 30°C.

Results and Discussion

CSTR and Direct Shear Tests

The data presented in Fig. 2 for the CSTR system treated with growing cells (initial inoculum of 10^3 live cfu/mL) show that the changes in pH, urea, and calcium correspond well with cell growth. For example, an increase in pH and decreases in calcium and urea values can be observed starting at 54 h and corresponding to a sharp change in the cell growth curve. These observations are consistent with Eqs. (1)–(4) and the findings reported by Fujita et al. (2000) and Bang et al. (2001). Similar trends were observed in the specimens inoculated with 10^7 cfu/mL; however, the increases in pH and cell numbers and decreases in calcium and urea values were observed earlier, starting at 18 h, probably owing to the greater inoculum size.

Specimens treated with growing cells were subjected to direct shear tests once the utilization rate of urea in the CSTR basin reached steady state (see Fig. 2). However, in the case of resting and dead cells, the cells were inoculated in the sand, and shear tests were performed after one day of curing time. This curing time was selected to give the cells enough time to attach to the surface of the sand particles, while minimizing the decay of the resting cells. Representative data from the direct shear test are presented in Figs. 3 and 4, and the strength parameters for the different specimens are summarized in Table 1. A common finding in all of the

J. Geotech. Geoenviron. Eng., 2011, 137(12): 1179-1189

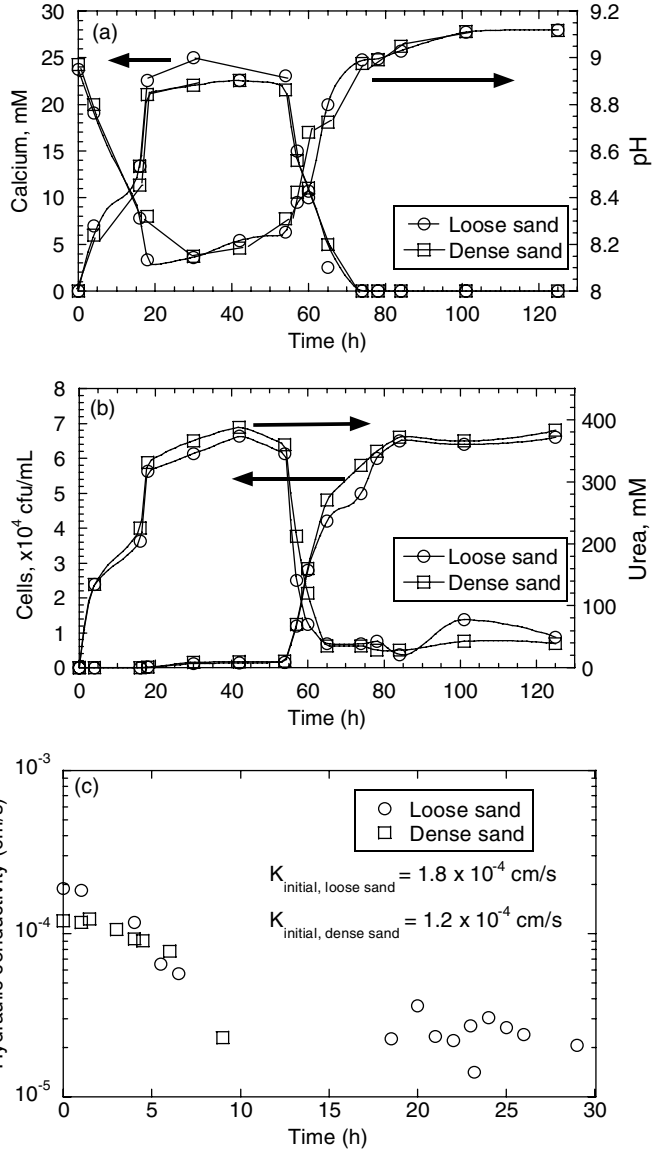

Fig. 2. Biotreatment of loose and dense sands by *S. pasteurii*: (a) temporal variations in calcium and pH; (b) temporal variations in urea and cell growth in CSTRs with an initial inoculum of 10^3 cfu/mL of bacteria; (c) hydraulic conductivity in CMBRs with an initial inoculum of 10^7 cfu/mL of bacteria

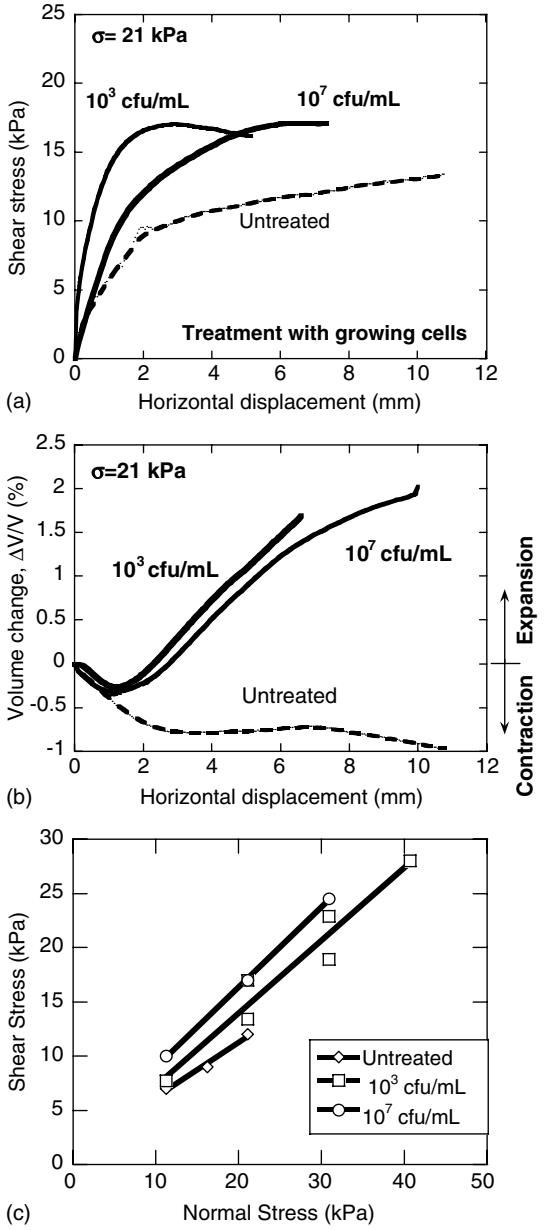

Fig. 3. (a) Stress-strain; (b) volume change–strain curves; (c) failure envelopes based on peak strength for untreated and biotreated sands (with growing cells inoculated at 10^3 or 10^7 cfu/mL) in direct shear tests at a relative density of 35%

results was that the peak strength increased with increasing normal stress [see Figs. 4(a) and 4(b)]. The typical stress-strain data in Fig. 3(a) illustrate the increase in the peak strength that was observed with the addition of growing cells for the loose sand at a normal stress of 21 kPa. The peak strength observed for the loose sand with the growing-cell treatment was generally greater than that observed for the other treatments. For example, at a normal stress of 21 kPa, the growing-cell treatments with the 10^3 cfu/mL and 10^7 cfu/mL inocula had 13% and 27% relative increases in peak strength, respectively, compared with the untreated sand. In comparison, the relative changes in peak strength with the dead and resting cells ranged, respectively, from 7.1% (10^3 cfu/mL) to 3.7% (10^7 cfu/mL), and from −28% (10^3 cfu/mL) to 8.2% (10^7 cfu/mL). The observation of increases in the peak strength of the loose sand with the growing-cell treatments is consistent with the findings of other studies of the microbiological treatment of concrete (Ramachandran et al. 2001) and naturally and artificially cemented sands (Clough et al. 1981). On the other hand, little or no improvement in peak strength was observed with any of the treatments for the dense sand. This is demonstrated in Fig. 4(c) for the dense sand treated with an initial inoculum of 10^7 CFU/mL of growing cells at a normal stress of 31 kPa. Similarly, relative increases in peak strength for the treated dense sand compared to the untreated sand ranged from −10% to 3.3% for all treatments at a normal stress of 21 kPa.

The volume change data in Fig. 3(b) indicate that volumetric expansion occurred during shear of the loose sand specimens treated with growing cells. As expected, the dense sand underwent a greater volume change than the loose sand, and the growing-cell treatments had larger volume changes than the dead and resting-cell treatments. The additional dilation with biotreatment is consistent

J. Geotech. Geoenviron. Eng., 2011, 137(12): 1179-1189

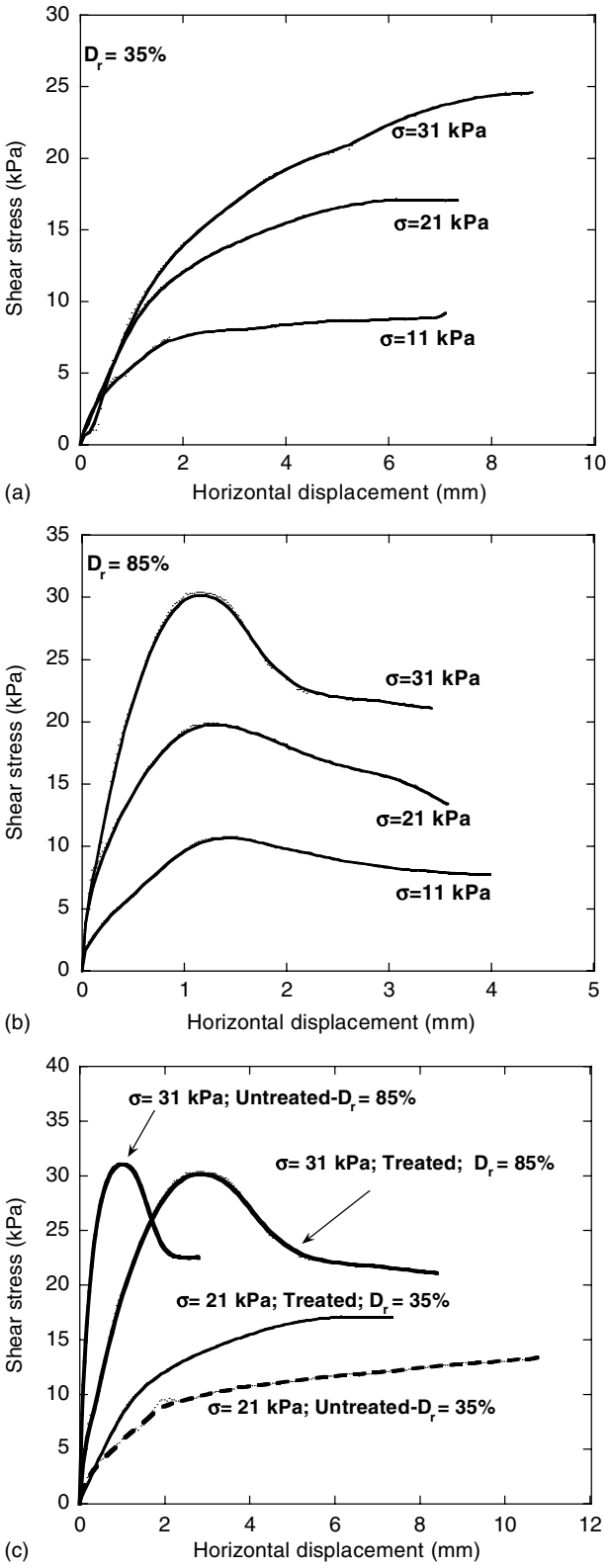

Fig. 4. Effect of normal stress on stress-strain behavior of biotreated (a) loose and (b) dense sands; (c) effect of biotreatment on loose and dense sands in direct shear tests; biotreatment was conducted with growing cells inoculated at 10^7 cfu/mL

with the findings of Clough et al. (1981) for naturally and artificially cemented sands.

Examples of peak strength envelopes for the untreated and biotreated loose sands are presented in Fig. 3(c), with friction angle and cohesion data based on the Mohr-Coulomb failure envelopes for all specimens summarized in Table 1. On the basis of these data, the untreated sands have friction angles consistent with those previously reported for poorly graded sands with loose and dense compactions (Bardet 1997; Ashford et al. 2002; FEMA 2005). In all cases tested, the friction angle also increased with increasing relative density and normal stress applied (see Table 1 and Fig. 4). This is probably attributable to the greater number of contacts per particle as the relative density increased and the void ratio decreased [e.g., Khan et al. (2006)]. For example, the average number of contacts per particle, i.e., the coordination number, varies almost linearly with the void ratio (Smith et al. 1929). Furthermore, the friction angles of the treated specimens, in general, increased compared to the untreated specimens, with the greatest increase for the loose and dense sands with the growing-cell treatment. Thus, the growing cell-treated sands have the more significant frictional component of strength, with larger friction angles for the dense sand. Friction angles of similar magnitude were observed in naturally cemented sands by Clough et al. (1981), who also observed an increase in friction angle with increasing relative density of artificially cemented sands. The results presented in Table 1 and Fig. 3(c) also show that a small amount of increase in cohesion was observed for almost all of the treatments. Clough et al. (1981) determined small residual cohesion values of similar magnitude (5–6 kPa) for artificially cemented sand with low (2% by weight) cement contents and with natural sands they deemed to be weakly cemented, although the peak cohesion values measured for those samples (12–46 kPa) were higher than those observed in this study. The authors attributed this small residual cohesion to capillary tension effects, or the presence of small quantities of cementing agents with strength of a ductile nature.

Improvements in the peak strength and friction angle of the loose sand with the growing-cell treatment can be attributed to the formation of precipitates (i.e., calcite or other calcareous crystals) induced by *S. pasteurii*, which may in turn cement the pore surfaces, as shown in previous studies (Ramachandran et al. 2001; Rodriguez-Navarro et al. 2003). As discussed previously, the growing *S. pasteurii* cells probably promoted the formation of calcium precipitates via development of a biofilm and production of EPS and by allowing the cation (e.g., Ca^{2+}) to be effectively adsorbed onto sand particles and form mineral deposits (Beveridge et al. 1997). However, when compared with the results for naturally and artificially cemented sands by Clough et al. (1981), the direct shear specimens would be categorized as weakly cemented. This is largely a product of the techniques used for preparing these specimens, which probably limited the amount of cementation.

Reasons for the changes observed in the specimens treated with dead and resting cells (see Table 1) are less clear, but there are several possible explanations. Dead cells have similarly been shown to absorb cations on the cell surface, which can also react with carbonate ions in solution (Greenfield 1963; Stocks-Fischer et al. 1999). Thus, $CaCO_3$ deposition is not directly dependent on the living state of the microorganisms, and the same mechanisms described above for growing cells may also be involved in case of dead and resting cells. However, in this study, the dead and resting cells were present in the CSTR in Tris-HCl buffer, not the urea-$CaCl_2$ medium, and it is unlikely that significant carbonate precipitation occurred under these conditions. Similarly, in their study of bacterially induced precipitation for concrete remediation, Ramachandran et al. (2001) observed increases in compressive strength in specimens treated with dead cells. They suggested that dead cells may act as organic fibers and thereby may contribute to strength. Again, it seems unlikely that this mechanism contributed significantly to the observed increases in strength and friction angle

J. Geotech. Geoenviron. Eng., 2011, 137(12): 1179-1189

Table 1. Direct Shear Test Results for Cohesion and Internal Friction Angles, of Specimens Prepared in Completely Stirred Tank Reactors

	Loose ($D_r = 35\%$)[a]				Dense ($D_r = 85\%$)							
	10^3 cfu/mL		10^7 cfu/mL		10^3 cfu/mL				10^7 cfu/mL			
Cell type	c	ϕ	c	ϕ	c_{peak}	ϕ_{peak}	$c_{residual}$	$\phi_{residual}$	c_{peak}	ϕ_{peak}	$c_{residual}$	$\phi_{residual}$
Dead cells	5.5	28	0.7	35	5.2	33	7.6	23	5.2	38	4.4	30
Resting cells	3.3	25	3.1	29	2.9	35	~0	34	3.1	40	2.4	30
Growing cells	1.0	34	1.2	38	5.2	39	0.6	37	1.0	43	1.3	34
Blank (0 cfu/mL)	$c \sim 0$; $\phi = 27°$				$c_{peak} \sim 0$; $\phi_{peak} = 33°$; $c_{residual} \sim 0$; $\phi_{residual} = 23°$							

Note: Cohesion is shown a c (in kPa), internal friction angle is shown as ϕ (in degrees).
[a]D_r = relative density.

with the resting or dead cells in the current study, given the small size of the cells compared to the sand particles. Another possible explanation for the strength increase is that the addition of the cells may have increased the dry unit weights of the specimens. Although not physically checked, this also seems unlikely to have a significant effect, given the small mass of dead and resting cells present. Thus, none of the possible explanations are expected to result in significant changes in strength, consistent with the previous observations.

Whether cells are serving as nucleation sites and inducing precipitation of calcareous crystals through their metabolic activities or contributing to changes in soil strength through some other mechanism, an increase in effect is expected with increased cell numbers. Correspondingly, the peak friction angle was observed to increase with increasing cell numbers for all the cell types, as summarized in Table 1.

CMBR and CBR Tests

In the CMBR systems inoculated with growing cells, the effluent trends in urea, pH, cell number, and calcium concentration were similar to those observed in the CSTR system and presented in Fig. 2. The calcium and urea concentrations initially increased as they were diluted into the system, and then decreased after approximately 20 h (data not shown). Therefore, dilution of those substrates was dominant between the first and second HRT, after which urea degradation and carbonate precipitation became dominant and the pH level increased. Calcium concentrations in both columns decreased to below the detection limit after 33–35 h, suggesting that microbially induced calcification was limited by the calcium concentration. After 33 h and 44 h in the loosely and densely compacted sand columns, respectively, the CMBR reactors were at steady state with respect to urea utilization and cell growth.

The cell growth and biocalcification resulted in increased head loss and decreased flow rate, as expected. Correspondingly, the hydraulic conductivity of the sand in both columns decreased from an initial value of $\sim 1 \times 10^{-4}$ cm/s to about 2×10^{-5} cm/s [see Fig. 2(c)]. For the dense and loose compactions, head loss became too large to measure with the piezometers after 10 and 30 h, respectively. Flow rate, however, was monitored until the head generated by the peristaltic pump controlling the influent rate was insufficient to overcome the head loss in the columns (i.e., $Q = 0$), which occurred after 80 h and 112 h of incubation in the dense- and loose-compaction columns, respectively.

CBR testing was performed on the specimens treated with growing cells after flow could no longer be generated through the column, whereas specimens with resting and dead cells were tested after preparation. The cell types and concentration and the degree of sand compaction all affected the CBR values, which are summarized in Table 2. Growing cells increased the CBR, especially in the case of dense sand, presumably owing to microbially induced precipitate formation (Ramachandran et al. 2001; DeJong et al. 2006). This precipitation process increased the CBR of the dense sand by up to 6.8 times with an inoculation of growing cells at 10^7 cfu/mL [see Fig. 5(a)], similar to the increase observed in shear testing of gypsum-cemented sands by DeJong et al. (2006). In comparison, an approximately twofold increase in CBR was observed in the loose sand under the same conditions. The higher relative density and increased number of contacts per particle with the dense sand probably contributed to the greater efficiency of biocementation with the growing-cell treatment.

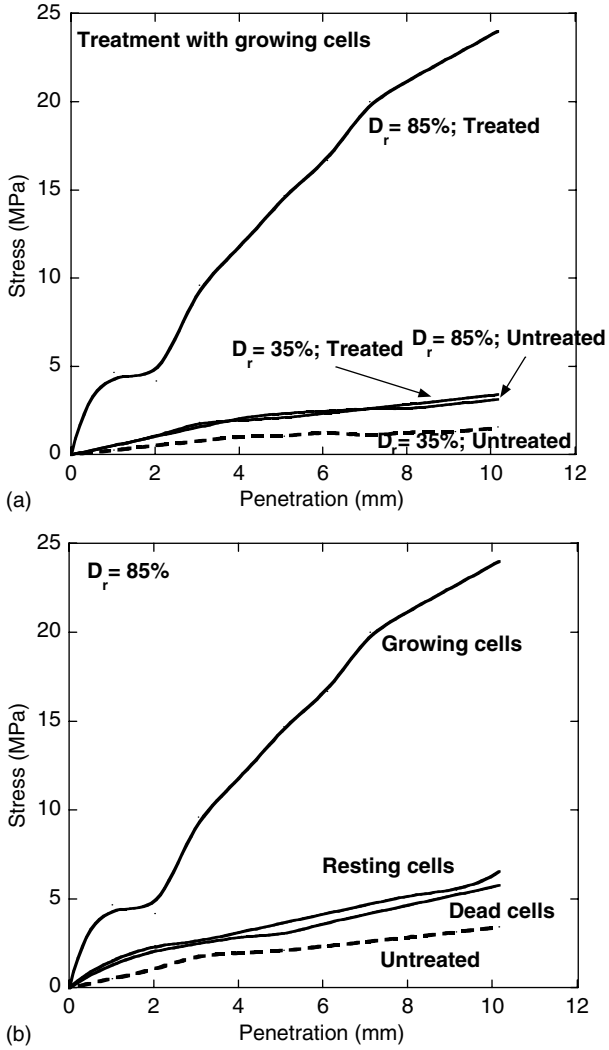

Fig. 5. Stress-penetration curves in CBR tests: (a) Effect of treatment and soil relative density on loose and dense sands; (b) effect of cell type on biotreated dense sands; biotreatment was conducted with an initial inoculum of 10^7 cfu/mL of bacteria

J. Geotech. Geoenviron. Eng., 2011, 137(12): 1179-1189

Table 2. California Bearing Ratio (%) of Specimens Prepared in Completely Mixed Biofilm Reactors

	Loose ($D_r = 35\%$)		Dense ($D_r = 85\%$)	
Cell type	10^3 cfu/mL	10^7 cfu/mL	10^3 cfu/mL	10^7 cfu/mL
Blank (0 cfu/mL)	10		21	
Dead cells	16	29	14	39
Resting cells	17	18	25	35
Growing cells	NA[a]	21	NA[a]	143

[a]NA = not analyzed.

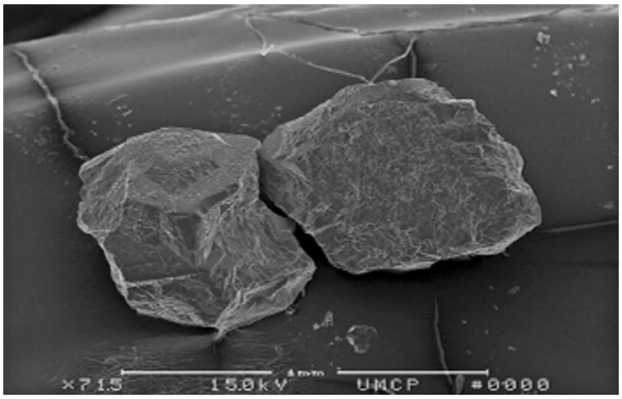

(a)

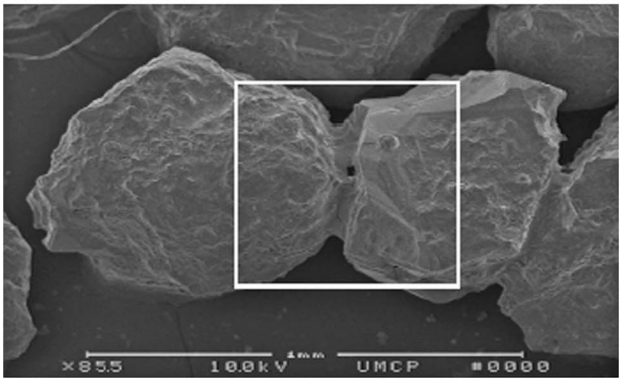

(b)

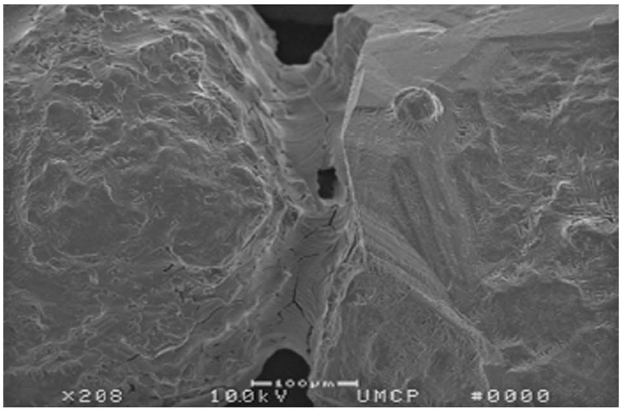

(c)

Fig. 6. SEMs of: (a) untreated sand with pretreatment before SEM analysis; (b) biocemented sand without pretreatment before SEM analysis; (c) focus on the area within the square boundary in panel (b) (images by authors)

The dead and resting cells, on the other hand, generally did not contribute as significantly to the CBR, as shown in Fig. 5(b). In addition, unlike observations with the dense sand treated with growing cells, the initial response to loading by the soils treated with dead and resting cells was stiff, with the soils exhibiting a softening behavior after 2.5- to 3-mm penetration of the piston, similar to the untreated soil. Increases in CBR with these treatments ranged from negligible to three times that of the loose and dense sand, with increases in the loose sand generally larger than in the dense sand (see Table 2). As discussed above, these negligible-to-small impacts observed with dead and resting cells may be a result of cells serving as nucleation sites or acting like organic fibers and thereby contributing to the overall strength of the treated sand; or the cell additions may have caused an increase in dry unit weights of the specimens. Again, none of these explanations seem likely to cause significant changes under the given experimental conditions, consistent with the relatively small changes observed.

As with friction angle, the CBR increased when the concentration of dead or resting cells increased, regardless of the relative density of the sand (see Table 2). For example, the CBRs of the loose and dense sands treated with 10^3 dead cfu/mL was about 16 and 14, respectively. In comparison, the loose- and dense-sand CBRs increased to about 29 and 39, respectively, when the bacterial concentration was increased to 10^7 cfu/mL.

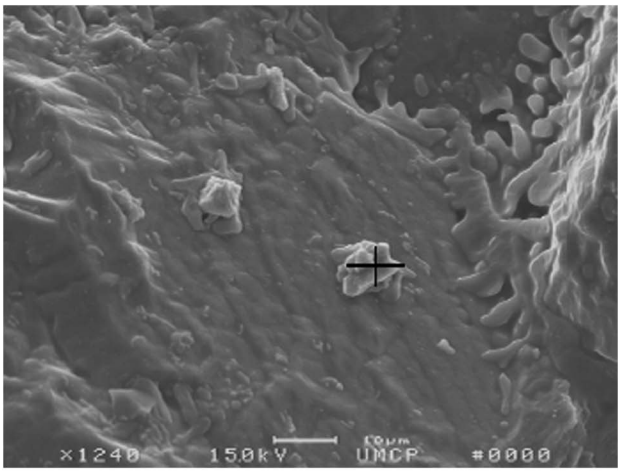

(a)

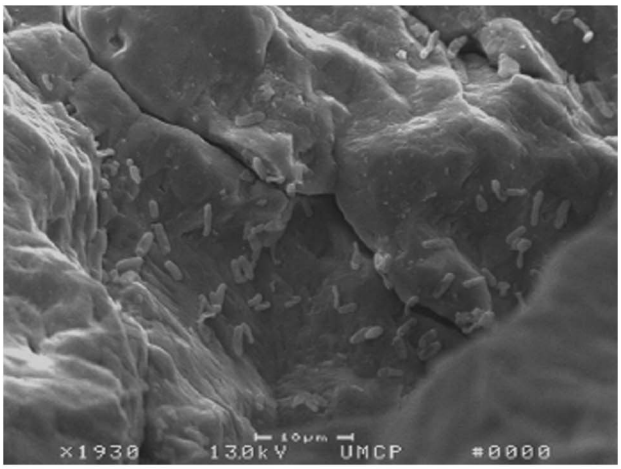

(b)

Fig. 7. SEMs of the surface of biotreated sand: (a) without and (b) with pretreatment before SEM analysis (images by authors)

J. Geotech. Geoenviron. Eng., 2011, 137(12): 1179-1189

Given that the greatest increase in CBR occurred in the CMBR with dense sand and growing cells inoculated at 10^7 cfu/mL, it was the focus of additional analysis. Porous media samples taken after the CBR test were found to have an average (inlet and outlet) of 0.40% VS by dry weight (g VS/g sand) ($s = 0.0086\%$) and 68.8% Ca as $CaCO_3$ (g $CaCO_3$/g sand) ($s = 0.212\%$). The inlet and outlet measurements were very similar, suggesting that these values were relatively uniform throughout the column as expected with the hydraulically completely mixed reactor. On the basis of the VS value, the biofilm thickness, $L_{f,a}$, was estimated at 0.056 mm [Eq. (5)], and the density, $X_{f,a}$, at 11.1 mg VS/cm^3 [Eq. (6)], whereas the calcium content was used to estimate an $L_{f,i}$ of 0.040 mm [Eq. (7)]. The biofilm thickness and inorganic solid film thickness estimates are similar in magnitude, despite the greater mass of calcium precipitates accumulated in the porous medium compared to the mass of VS, because the density of the inorganic solid film is expected to be much greater than the volatile film density (VanGulck and Rowe 2004b).

Although useful, as outlined subsequently, a number of approximations have been associated with these film thickness estimates. For example, the estimation of the sand grain surface area affected all three values. Also, in the biofilm measurements, it is not possible to distinguish water adhering to mineral precipitate/sand from water in the biomass (VanGulck and Rowe 2008), which would tend to overestimate $L_{f,a}$ and thereby underestimate $X_{f,a}$. Similarly, the assumed density of calcite for the inorganic precipitate in the calculation of $L_{f,i}$ may not be the actual value, which would affect the estimate for $L_{f,i}$. Nonetheless, the estimated film thicknesses do suggest that biomass growth and mineral precipitation contributed significantly to the reduction in the pore space of the porous medium.

To evaluate the loss of porosity attributable to the film accumulation in the CMBR, the total estimated film thickness, L_t ($= L_{f,a} + L_{f,i}$) was normalized to the particle diameter, d_p (assumed to equal the D_{50}), as $(2L_t/d_p)$, following the approach of Cooke and Rowe (1999) and resulting in a value of 0.42. On the basis of the estimated porosity of 0.42 for the densely compacted sand, it was calculated that there were approximately eight contacts per sand particle (Smith et al. 1929) and, therefore, assumed that the packing approximated an orthorhombic arrangement. According to the analysis of Cooke and Rowe (1999) for orthorhombic packing, clogging of spherical porous media occurs when the porosity is reduced to 10% of the original value, corresponding to a value of $(2L_t/d_p) = 0.31$, and complete pore occlusion when $(2L_t/d_p) = 0.5275$. The estimated value of 0.42 for this study falls within this range, consistent with the observed loss of hydraulic conductivity discussed previously.

Although the biofilm and inorganic solid film estimates are useful for comparing the relative contributions of biomass and mineral

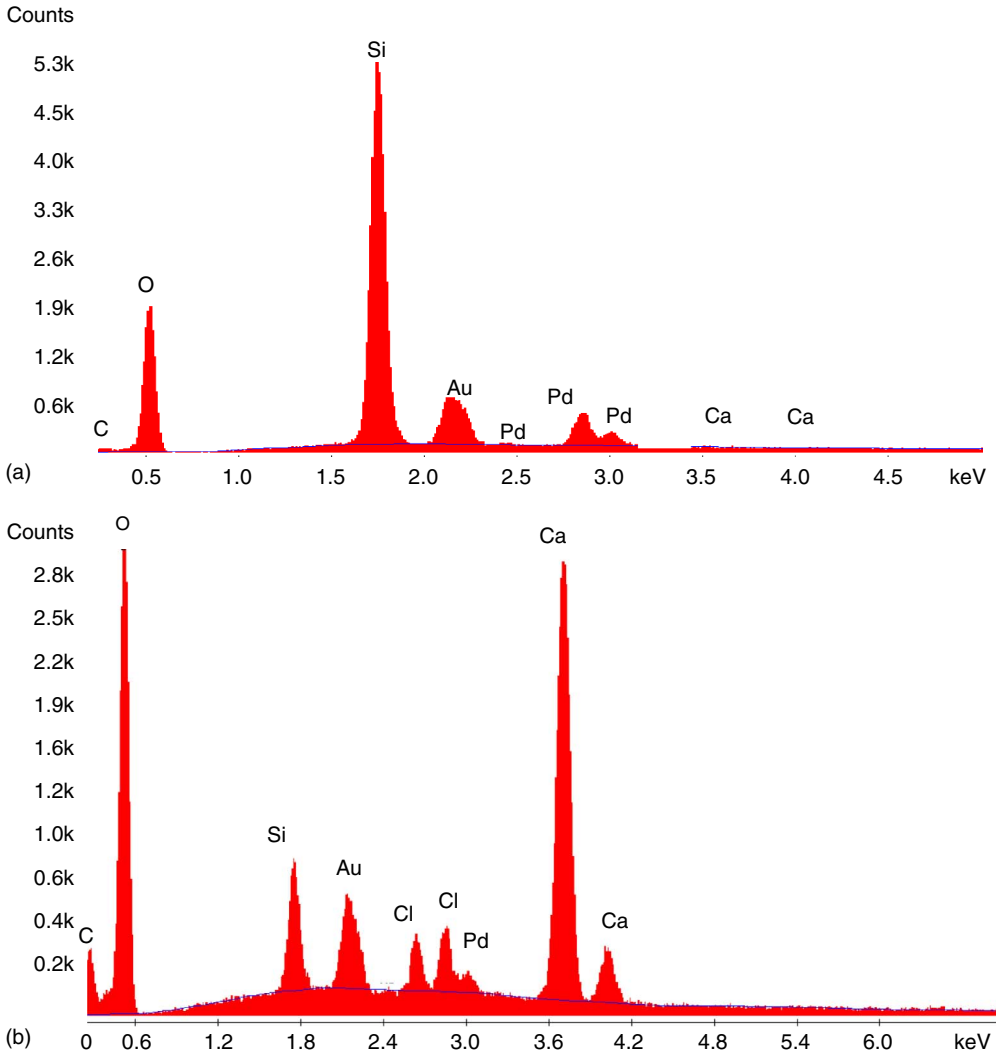

Fig. 8. Composite profile: (a) untreated sand grains; (b) growing cell-treated sand grains by using EDS

J. Geotech. Geoenviron. Eng., 2011, 137(12): 1179-1189

precipitate to clogging, they do not provide any insight into the actual in situ structure of the clog material (VanGulck and Rowe 2004a). Therefore, SEM and EDS analyses were performed on untreated sand and CMBR specimens subjected to microbial treatment with growing cells (initial inoculum $= 10^7$ cfu/mL) in the CBR columns. In comparison to the untreated sand [see Fig. 6(a)], the microbiologically treated specimens showed evidence of cementation on the particle surface and at particle contacts as shown in Figs. 6(b) and 6(c). The images in Fig. 6 and others available at Chou et al. (2008) demonstrate significant bonding at most particle contact points, comparable to the intermediate cementation levels described by Chang and Woods (1992). Crystal faces formed as a result of treatment with *S. pasteurii* are apparent in the highly magnified images [e.g., Fig. 7(a)], similar to observations made by DeJong et al. (2006). As shown in Fig. 7(b), pretreatment before the SEM analysis to remove the heavy cementation revealed the bacterial attachment to the sand particles, consistent with the findings of Fujita et al. (2000) and Bang et al. (2001).

Further confirmation of the biocalcification was obtained by analyzing for the presence of calcium crystals through EDS coupled with SEM. On the basis of the EDS analysis performed on magnified SEM images of untreated and treated (see Fig. 8) specimens, the compositional profile of the crystal on the surface of the treated sand grains had a high Ca content relative to the profile of the untreated sand, which had none, further indicating that cementation was the result of microbially induced precipitation of calcium minerals, presumably calcite (Stocks-Fischer et al. 1999). Thus, the overall results of the SEM and EDS analyses confirm the biofilm and inorganic film evaluations indicating that the clogging of the pore space in the sand resulted from a combination of biomass growth and calcium precipitates.

It should be acknowledged that the CBR specimens were allowed to free drain before the tests, and thus the tests were conducted on unsaturated specimens. The decrease in porosity associated with clogging of the pore space by a combination of biomass and calcium precipitates may have resulted in an increase in soil suction (negative pore pressure) in the unsaturated specimens, thereby contributing to the increase in CBR values. However, no data were collected on this point.

Conclusions

The hydrolysis of urea was promoted in CSTR and CMBR systems containing loose- or dense-sand specimens that were inoculated with growing *S. pasteurii* cells. As a result, an increase in pH to 9.1 was observed, thereby creating a favorable environment for $CaCO_3$ precipitation. Other specimens were treated with dead and resting *S. pasteurii* cells. Specimens prepared in the CSTR and CMBR systems were subjected to direct shear and CBR tests, respectively. In the direct shear tests, the peak strength observed for the loose sand with the growing-cell treatment was generally greater than for the other treatments. Furthermore, the friction angles of all of the treated specimens generally increased compared to the untreated specimens, with the greatest increase for the growing-cell treatment, and a small increase in cohesion was observed for almost all treatments. Growing cells also increased the CBR, especially in case of the dense sand. The dead and resting cells, on the other hand, generally did not contribute as significantly to the CBR. Treatment with growing cells also resulted in a decrease in the hydraulic conductivity of loose- and dense-sand columns. Evaluation of the VS and calcium associated with the sand particles, coupled with SEM and EDS analyses, suggests that biomass growth and calcium mineral precipitation contributed significantly to clogging of the porous medium. The increase in biofilm and mineral films in specimens treated with growing cells was attributable to the microbial activity, which induced conditions conducive for the precipitation of calcium minerals, presumably calcium carbonate.

Acknowledgments

This material is based upon work supported by the National Science Foundation under Grant No. CMS-05-28171. Any opinions, findings, and conclusions or recommendations expressed in this material are those of the writers and do not necessarily reflect the views of the National Science Foundation. The writers acknowledge Professor Sookie S. Bang (South Dakota School of Mines and Technology, Rapid City, SD, USA) for providing the original *Sporosarcina pasteurii* strain 11859 culture used in these experiments.

References

Abd-El-Malek, Y., and Rizk, S. G. (1963). "Bacterial sulphate reduction and the development of alkalinity. II. Laboratory experiments with soils." *J. Appl. Bacteriol.*, 26(1), 14–19.

Abdelouas, A., Lu, Y. M., Lutze, W., and Nuttall, H. E. (1998). "Reduction of U(VI) to U(IV) by indigenous bacteria in contaminated ground water." *J. Contam. Hydrol.*, 35(1–3), 217–233.

Abdulla, W. A. (1995). "Centrifuge modeling of sinkhole development in weakly cemented sand." Ph.D. dissertation, Univ. of Maryland, College Park, MD.

Aloisi, G., Gloter, A., Kroger, M., Wallmann, K., Guyot, F., and Zuddas, P. (2006). "Nucleation of calcium carbonate on bacterial nanoglobules." *Geology : J. Association of Teachers of Geol.*, 34(12), 1017–1020.

American Public Health Association (APHA), American Water Works Association (AWWA), and Water Environment Federation (WEF). (1995). *Standard methods for the examination of water and wastewater.* 19th Ed., Washington, DC.

Ashford, S. A., Weaver, T. J., and Rollins, K. M. (2002). "Pore pressure response of liquefied sand in full-scale lateral pile load tests." *Transportation Research Record 1808*, Transportation Research Board, Washington, DC, , 21–29.

ASTM. (2005). "Standard test method for direct shear test of soils under consolidated drained conditions." *D3080*, West Conshohocken, PA.

Bang, S. S., Galinat, J. K., and Ramakrishnan, V. (2001). "Calcite precipitation induced by polyurethane-immobilized *Bacillus pasteurii*." *Enzyme and microbial technology*, 28(4–5), 404–409.

Bardet, J. P. (1997). *Experimental soil mechanics*, Prentice-Hall, Upper Saddle River, NJ.

Beveridge, T. J., Makin, S. A., Kadurugamuwa, J. L., and Li, Z. S. (1997). "Interactions between biofilms and the environment." *FEMS Microbiol. Rev.*, 20(3–4), 291–303.

Braissant, O., Decho, A. W., Dupraz, C., Glunk, C., Przekop, K. M., and Visscher, P. T. (2007). "Exopolymeric substances of sulfate-reducing bacteria: Interactions with calcium at alkaline pH and implication for formation of carbonate minerals." *Geobiology*, 5(4), 401–411.

Buczynski, C., and Chafetz, H. S. (1991). "Habit of bacterially induced precipitates of calcium-carbonate and the influence of medium viscosity on mineralogy." *J. Sediment. Res.*, 61(2), 226–233.

Castanier, S., Le Metayer-Levrel, G., and Perthulsot, J. P. (1999). "Ca-carbonates precipitation and limestone genesis: The microbiogeologist point of view." *Sediment. Geol.*, 126(1–4), 9–23.

Chang, T. S., and Woods, R. D. (1992). "Effect of particle contact bond on shear modulus." *J. Geotech. Eng.*, 118(8), 1216–1233.

Chou, C.-W. (2008). "Biomodification of geotechnical properties of sand." M.S. thesis, Univ. of Maryland, College Park, MD.

Chou, C.-W., Seagren, E. A., Aydilek, A. H., and Maugel, T. K. (2008). "Bacterially-induced calcite preciptation via ureolysis." *ASM Microbe-Library, Visual Resource Collection*, American Society for Microbiology, Washington, DC ⟨http://www.microbelibrary.org/⟩.

Clough, G. W., Sitar, N., Bachus, R. C., and Rad, N. S. (1981). "Cemented sands under static loading." *J. Geotech. Engrg. Div.*, 107(6), 799–817.
Cooke, A. J., and Rowe, R. K. (1999). "Extension of porosity and surface area models for uniform porous media." *J. Environ. Eng.*, 125(2), 126–136.
Day, J. L., Ramakrishnan, V., and Bang, S. S. (2003). "Microbiologically induced sealant for concrete crack remediation." *Proc., 16th Engineering Mechanics Conf.*, ASCE, Reston, VA.
Defarge, C., Trichet, J., Jaunet, A. M., Robert, M., Tribble, J., and Sansone, F. J. (1996). "Texture of microbial sediments revealed by cryo-scanning electron microscopy." *J. Sediment. Res.*, 66(5), 935–947.
DeJong, J. T., Fritzges, M. B., and Nusslein, K. (2006). "Microbially induced cementation to control sand response to undrained shear." *J. Geotech. Geoenviron. Eng.*, 132(11), 1381–1392.
DeJong, J. T., Mortensen, B. M., Martinez, B. C., and Nelson, D. C. (2010). "Biomediated soil improvement." *Ecol. Eng.*, 36(2), 197–210.
Ehrlich, H. L. (2002). *Geomicrobiology*, Marcel Dekker, New York.
Ercole, C., Cacchio, P., Botta, A. L., Centi, V., and Lepidi, A. (2007). "Bacterially induced mineralization of calcium carbonate: The role of exopolysaccharides and capsular polysaccharides." *Microsc. Microanal.*, 13(1), 42–50.
FEMA. (2005). *Coastal construction manual: Principles and practices of planning, siting, designing, constructing, and maintaining residential buildings in coastal areas*, Federal Emergency Management Agency, Washington, DC.
Ferris, F. G., Phoenix, V., Fujita, Y., and Smith, R. W. (2004). "Kinetics of calcite precipitation induced by ureolytic bacteria at 10 to 20 degrees C in artificial groundwater." *Geochim. Cosmochim. Acta*, 68(8), 1701–1710.
Fujita, Y., Ferris, E. G., Lawson, R. D., Colwell, F. S., and Smith, R. W. (2000). "Calcium carbonate precipitation by ureolytic subsurface bacteria." *Geomicrobiol. J.*, 17(4), 305–318.
Gollapudi, U., Knutson, C., Bang, S. S., and Islam, M. (1995). "A new method for controlling leaching through permeable channels." *Chemosphere*, 30(4), 695–705.
Greenfield, L. J. (1963). "Metabolism and concentration of calcium and magnesium and precipitation of calcium carbonate by a marine bacterium." *Ann. N.Y. Acad. Sci.*, 109(1), 23–45.
Jung, D., Biggs, H., Erikson, J., and Ledyard, P. U. (1975). "New colorimetric reaction for endpoint, continuous-flow, and kinetic measurement of urea." *Clin. Chem.*, 21(8), 1136–1140.
Karatas, I., Kavazanjian, E. Jr., and Rittman, B. E. (2008). "Microbially induced precipitation of calcite using Pseudomonas denitrificans." *1st Int. Conf. on BioGeo Civil Engineering*, Deltares and Delft Univ. of Technology, Delft, The Netherlands.
Khan, Z., Majid, A., Cascante, G., Hutchinson, D. J., and Pezeshkpour, P. (2006). "Characterization of a cemented sand with the pulse-velocity method." *Can. Geotech. J.*, 43(3), 294–309.
Krumbein, W. C. (1941). "Measurement and geological significance of shape and roundness of sedimentary particles." *J. Sediment. Res.*, 11(2), 64–72.
Lee, K. C., and Rittmann, B. E. (2003). "Effects of pH and precipitation on autohydrogenotrophic denitrification using the hollow-fiber membrane-biofilm reactor." *Water Res.*, 37(7), 1551–1556.
Mitchell, A. C., and Ferris, F. G. (2006). "The influence of *Bacillus pasteurii* on the nucleation and growth of calcium carbonate." *Geomicrobiol. J.*, 23(3–4), 213–226.
Monger, H. C., Daugherty, L. A., Lindemann, W. C., and Liddell, C. M. (1991). "Microbial precipitation of pedogenic calcite." *Geology*, 19(10), 997–1000.
National Research Council (NRC). (2006). *Geological and geotechnical engineering in the new millennium*, National Academies Press, Washington, DC.
Ramachandran, S. K., Ramakrishnan, V., and Bang, S. S. (2001). "Remediation of concrete using microorganisms." *ACI Mater. J.*, 98(1), 3–9.
Rittmann, B. E., Banaszak, J. E., Cooke, A., and Rowe, R. K. (2003). "Biogeochemical evaluation of mechanisms controlling $CaCO_3$(s) precipitation in landfill leachate-collection systems." *J. Environ. Eng.*, 129(8), 723–730.
Roberts, W. L., Campbell, T. J., and Rapp, G. R. Jr. (1990). *Encyclopedia of minerals*, 2nd Ed., Van Nostrand Reinhold, New York.
Rodriguez-Navarro, C., Rodriguez-Gallego, M., Ben Chekroun, K., and Gonzalez-Munoz, T. (2003). "Conservation of ornamental stone by Myxococcus xanthus-induced carbonate biomineralization." *Appl. Environ. Microbiol.*, 69(4), 2182–2193.
Ross, N., Villemur, R., Deschênes, L., and Samson, R. (2001). "Clogging of limestone fracture by stimulating groundwater microbe." *Water Res.*, 35(8), 2029–2037.
Rowe, R. K., VanGulck, J. F., and Millward, S. C. (2002). "Biologically induced clogging of a granular medium permeated with synthetic leachate." *J. Environ. Eng. Sci.*, 1(2), 135–156.
Russell, R. D., and Taylor, R. E. (1937). "Roundness and shape of Mississippi River sands." *J. Geol.*, 45(3), 225–267.
Sawyer, C., McCarty, P. L., and Parkin, G. (2003). *Chemistry for environmental engineering and science*, McGraw-Hill, Boston.
Schultze-Lam, S., Fortin, D., Davis, B. S., and Beveridge, T. J. (1996). "Mineralization of bacterial surfaces." *Chem. Geol.*, 132(1–4), 171–181.
Seagren, E. A., and Aydilek, A. H. (2010). "Biomediated geomechanical processes." Chapter 24, *Environmental microbiology*, 2nd Ed., R. Mitchell, and J.-D. Gu, eds., Wiley, Hoboken, NJ, 319–348.
Seagren, E. A., Rittmann, B. E., and Valocchi, A. J. (2002). "Bioenhancement of NAPL pool dissolution: Experimental evaluation." *J. Contam. Hydrol.*, 55(1–2), 57–85.
Smith, W. O., Foote, P. D., and Busang, P. F. (1929). "Packing of homogeneous spheres." *Phys. Rev.*, 34(9), 1271–1274.
Stocks-Fischer, S., Galinat, J. K., and Bang, S. S. (1999). "Microbiological precipitation of $CaCO_3$." *Soil Biol. Biochem.*, 31(11), 1563–1571.
Thompson, J. B., and Ferris, F. G. (1990). "Cyanobacterial precipitation of gypsum, calcite, and magnesite from natural alkaline lake water." *Geology*, 18(10), 995–998.
Urzi, C., Garcia-Valles, M., Vendrell, M., and Pernice, A. (1999). "Biomineralization processes on rock and monument surfaces observed in field and in laboratory conditions." *Geomicrobiol. J.*, 16(1), 39–54.
Van Lith, Y., Warthmann, R., Vasconcelos, C., and McKenzie, J. A. (2003). "Microbial fossilization in carbonate sediments: A result of the bacterial surface involvement in dolomite precipitation." *Sedimentology*, 50(2), 237–245.
VanGulck, J. F., and Rowe, R. K. (2004a). "Evolution of clog formation with time in columns permeated with synthetic landfill leachate." *J. Contam. Hydrol.*, 75(1–2), 115–139.
VanGulck, J. F., and Rowe, R. K. (2004b). "Influence of landfill leachate suspended solids on clog (biorock) formation." *Waste Manage.*, 24(7), 723–738.
VanGulck, J. F., and Rowe, R. K. (2008). "Parameter estimation for modelling clogging of granular medium permeated with leachate." *Can. Geotech. J.*, 45(6), 812–823.
VanGulck, J. F., Rowe, R. K., Rittmann, B. E., and Cooke, A. J. (2003). "Predicting biogeochemical calcium precipitation in landfill leachate collection systems." *Biodegradation*, 14(5), 331–346.
Whiffin, V. S., van Paassen, L. A., and Harkes, M. P. (2007). "Microbial carbonate precipitation as a soil improvement technique." *Geomicrobiol. J.*, 24(5), 417–423.

J. Geotech. Geoenviron. Eng., 2011, 137(12): 1179-1189